

Primary transcripts of microRNAs encode regulatory peptides

Dominique Lauressergues^{1,2}, Jean-Malo Couzigou^{1,2}, H  l  ne San Clemente^{1,2}, Yves Martinez³, Christophe Dunand^{1,2}, Guillaume B  card^{1,2} & Jean-Philippe Combier^{1,2}

MicroRNAs (miRNAs) are small regulatory RNA molecules that inhibit the expression of specific target genes by binding to and cleaving their messenger RNAs or otherwise inhibiting their translation into proteins¹. miRNAs are transcribed as much larger primary transcripts (pri-miRNAs), the function of which is not fully understood. Here we show that plant pri-miRNAs contain short open reading frame sequences that encode regulatory peptides. The pri-miR171b of *Medicago truncatula* and the pri-miR165a of *Arabidopsis thaliana* produce peptides, which we term miPEP171b and miPEP165a, respectively, that enhance the accumulation of their corresponding mature miRNAs, resulting in downregulation of target genes involved in root development. The mechanism of miRNA-encoded peptide (miPEP) action involves increasing transcription of the pri-miRNA. Five other pri-miRNAs of *A. thaliana* and *M. truncatula* encode active miPEPs, suggesting that miPEPs are widespread throughout the plant kingdom. Synthetic miPEP171b and miPEP165a peptides applied to plants specifically trigger the accumulation of miR171b and miR165a, leading to reduction of lateral root development and stimulation of main root growth, respectively, suggesting that miPEPs might have agronomical applications.

The biogenesis of miRNAs involves two maturation steps: processing of large pri-miRNAs to shorter pre-miRNAs, and their subsequent maturation to produce active, mature miRNAs¹. Whether the pri-miRNAs themselves have a regulatory function is not known. Like protein-encoding mRNAs, pri-miRNAs are synthesized by RNA polymerase II¹; therefore, we hypothesized that they might also encode proteins or peptides. To test this hypothesis, we studied the miR171 family in the model plant *Medicago truncatula*, because we have previously documented the role of one of its members (miR171h) in mycorrhization². Here we selected miR171b for further analysis because it regulates the formation of lateral roots, a more easily monitored developmental step. We first identified the primary transcript of miR171b by performing a rapid amplification of cDNA ends (RACE)-PCR analysis (Extended Data Fig. 1). The DNA sequence surrounding the miR171b of 284 ecotypes of *M. truncatula*, (<http://www.medicagohapmap.org>) were compared for single-nucleotide polymorphism (SNP). As expected, the regions corresponding to the pre-miRNA, the miRNA and its partially complementary sequence miRNA* were highly conserved, with only 0.85% of SNPs in the pre-miRNA sequence, and none in the miRNA and in the miRNA* sequences (Extended Data Table 1). By contrast, the promoter and 3' region of the pri-miRNA were much more divergent (8.07% and 15.06% of SNPs, respectively; Extended Data Table 1), whereas the sequence of the 5' part of the pri-miRNA was more conserved (3.1% of SNPs), suggesting a functional constraint for coding regions. In support of our hypothesis, we identified two putative open reading frames (ORFs) potentially encoding peptides of 20 and 5 residues in this region of the pri-miR171b (Extended Data Fig. 1).

To investigate whether the start codons of the two putative ORFs are active, we fused the β -glucuronidase reporter gene *GUS* to the promoter region of the pri-miR171b. This region was sufficient to confer expression

specifically at lateral root initiations (Fig. 1a and Extended Data Fig. 2a–c). We next fused the *GUS* and the promoter region before either one of the two ATG and observed that only the first ATG drove the translation of the reporter gene at these sites (Fig. 1b); no translation was detected when *GUS* was placed downstream of the second ATG (Fig. 1c). Finally, we fused the promoter region and the first ORF (ORF1) to *GUS* and observed translation of this small ORF where lateral roots initiated (Fig. 1d and Extended Data Fig. 2d–f), demonstrating that ORF1 is translated in the plant.

To detect the endogenously produced peptide encoded by ORF1 in *M. truncatula*, we produced an antibody against this peptide. Immunofluorescence microscopy using this antibody indicated the presence of the peptide in lateral root initiations (Fig. 1e, f and Extended Data Fig. 2g-r), suggesting co-expression of the pri-miRNA. Immunoblotting showed that this antibody is highly specific for the peptide and that the peptide is produced naturally in *M. truncatula* roots (Fig. 1g). We call this miRNA-encoded peptide miPEP171b.

To investigate the possible regulatory role of miPEP171b in miR171b production, we used transformation of tobacco leaves³ to express native and mutant forms of *M. truncatula* pri-miR171b. In contrast to the large amount of miR171b produced by expression of the native pri-miR171b (Fig. 2a), expression of a mutant in which ORF1 was deleted produced smaller amounts of miR171b (Fig. 2a). Likewise, expression of a pri-miR171b in which the ATG start codon of ORF1 was mutated to ATT also produced smaller amounts of miR171b than did expression of the native pri-miR171b (Fig. 2a). This suggests that miPEP171b enhances the accumulation of its corresponding miRNA. To test this hypothesis further, we expressed the pri-miR171b together with the miPEP171b or with a control. The miR171b was more abundant when co-expressed with miPEP171b than with the control (Fig. 2b). Mutation of the start codon of the miPEP171b ORF from ATG to ATT abolished this enhanced accumulation of miR171b (Fig. 2b). Finally, a mutated miPEP171b ORF in which most nucleotides were changed without modifying the amino acid sequence of the peptide retained its positive effect on the accumulation of miR171b, reinforcing the conclusion that the ORF sequence acts as a peptide, not as an RNA (Fig. 2b).

To test whether miPEP171b enhances accumulation of miR171b in *M. truncatula*, we overexpressed miPEP171b in *M. truncatula* roots. This led to increased accumulation of endogenous miR171b (Fig. 2c). Also, overexpression of miPEP171b reduced lateral root density to a similar extent as did overexpression of pri-miR171b (Extended Data Fig. 3). Finally, overexpression of miPEP171b had no effect on the expression of other miRNAs we analysed, suggesting that miPEPs are active specifically on their respective miRNAs (Extended Data Fig. 4a).

We next investigated whether a synthetic miPEP171b applied exogenously would modify the expression of miR171b, and consequently modify plant development. The addition of miPEP171b to *M. truncatula* seedlings increased the abundance of miR171b (Fig. 2d), with consequent reduction of lateral root formation (Extended Data Fig. 3c). Treatment with a control peptide, with the same amino acid composition

¹Université de Toulouse, UPS, UMR5546, Laboratoire de Recherche en Sciences Végétales, 31326 Castanet-Tolosan, France. ²Centre National de la Recherche Scientifique, CNRS, UMR5546, 31326 Castanet-Tolosan, France. ³Fédération de Recherches FR3450 CNRS, 31326 Castanet-Tolosan, France.

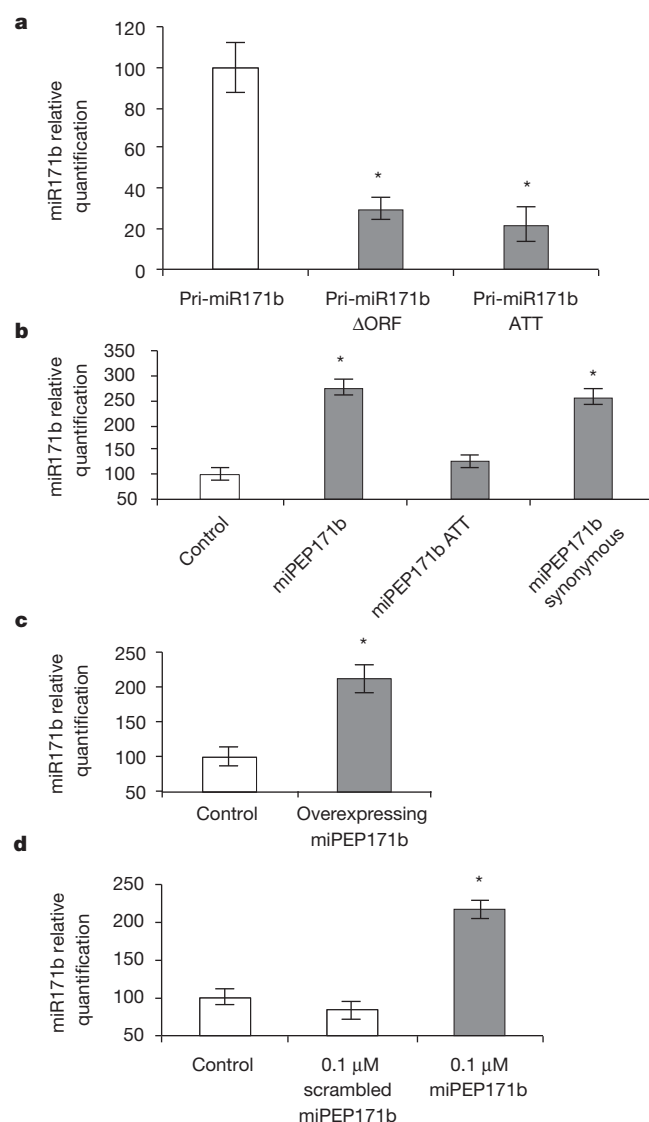
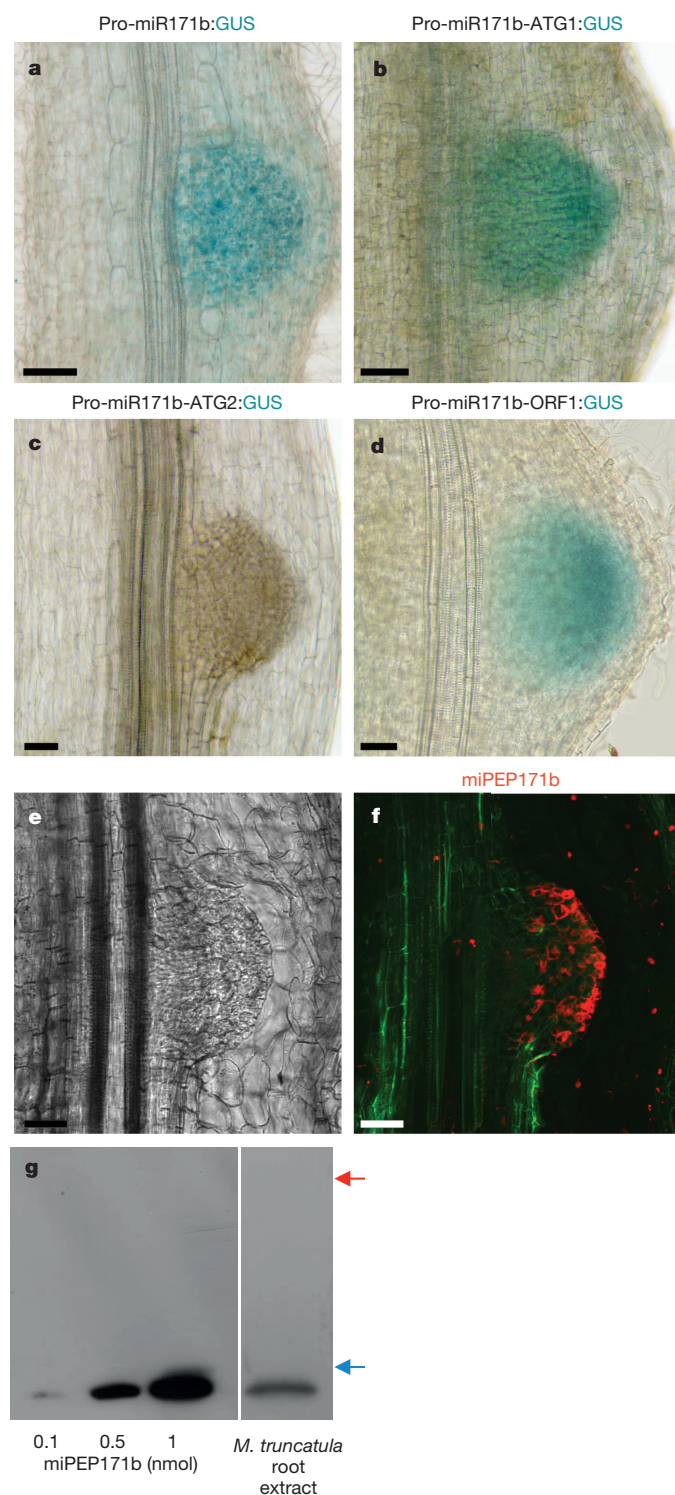


Figure 2 | Effect of miPEP171b on accumulation of miR171b.

a, Quantification of miR171b in tobacco leaves expressing the pri-miR171b, or the pri-miR171b in which the ORF1 was deleted (Δ ORF), or in which the ORF1 start codon was mutated to ATT. **b**, Quantification of miR171b in tobacco leaves expressing the pri-miR171b and a control, or the native miPEP171b, or a miPEP171b in which the ORF1 start codon was mutated to ATT, or in which the ORF1 nucleotide sequence was mutated without modifying the amino acid sequence (synonymous). **c**, Quantification of miR171b in control and miPEP171b-overexpressing *M. truncatula* roots. **d**, Quantification of miR171b in *M. truncatula* roots treated with solvent (control), synthetic scrambled or miPEP171b peptides. (Error bars, s.e.m.; asterisks, significant difference according to Student's *t*-test (**a, b**) or a Kruskal–Wallis test (**c, d**); $n = 30$ leaves or $n = 10$ roots, $P < 0.05$.)

as the miPEP171b but a scrambled sequence, had no effect (Fig. 2d). Finally, exogenous application of miPEP171b had no effect on other *M. truncatula* miRNAs (Extended Data Fig. 4b).

To see whether plant pri-miRNAs generally encode miPEPs, we analysed the data from ref. 4, which contain the sequences of the 5' ends of 50 pri-miRNAs in *Arabidopsis thaliana*. All of these pri-miRNAs contained at least one putative ORF, the 5'-most ORFs encoding peptides of 3–59 amino acid residues, without any indication of biological evidence (Extended Data Table 2). We found no common signature among them, suggesting each of these putative miPEPs is likely specific for its miRNA (Extended Data Table 2).

We next examined whether the miPEP encoded by pri-miR165a of *A. thaliana* might have similar regulatory functions in this plant as

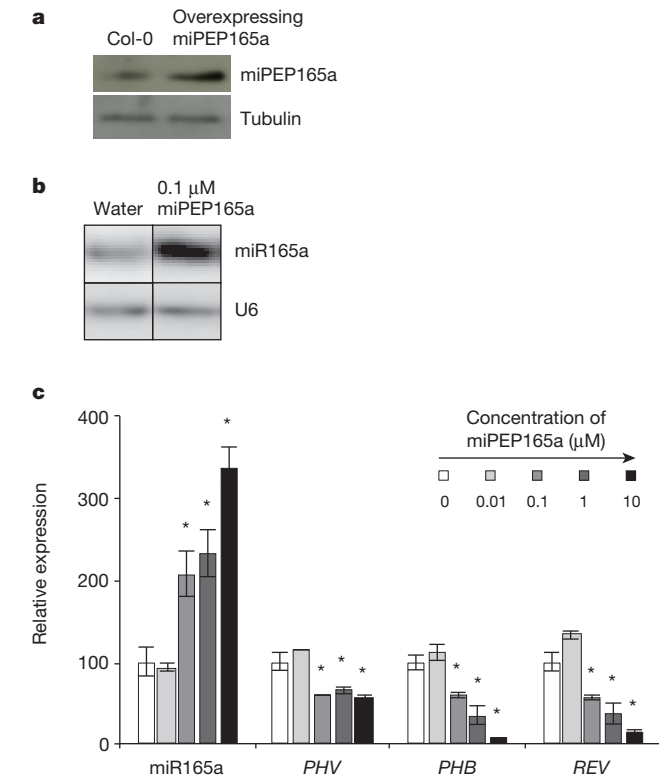


Figure 3 | Expression and effect of *A. thaliana* miPEP165a.

a, Immunoblotting of miPEP165a in wild-type (Col-0) and in miPEP165a overexpressing seedlings. **b**, Northern blot analysis of miR165a in seedlings treated with water or with synthetic miPEP165a. (**a**, **b**, see full scan blots in Supplementary Information.) **c**, Quantification of miR165a and of its target genes (*PHAVOLUTA* (*PHV*), *PHABOLUSA* (*PHB*) and *REVOLUTA* (*REV*))⁵ in seedlings treated with water or with synthetic miPEP165a. Darker bars represent increasing concentration of miPEP165a. One representative experiment of three (**a**) or four (**b**) performed is shown. Error bars, s.e.m.; asterisks, significant difference according to a Kruskal–Wallis test; $n = 10$ seedlings, $P < 0.05$.

those of the miPEP171b in *M. truncatula*. This miRNA is normally expressed in the root endodermis cells⁵. Notably, the miPEP165a amino acid sequence is well conserved in Brassicales (Extended Data Fig. 5). We first expressed fusions between the *GUS*-*GFP* and the promoter region before the first ATG or before putative alternative start codons CTG and GTG of pri-miR165a in *A. thaliana* (Extended Data Fig. 6a). The first ATG was active in endodermis cells, whereas the CTG and GTG codons were not active, indicating that the ATG is the functional start codon of this peptide (Extended Data Fig. 6b–f). Notably, the ribosome footprint data of ref. 6 revealed that the sequence encoding miPEP165a in pri-miR165a is occupied by ribosomes in *A. thaliana* seedlings, strongly suggesting that this sequence is translated (data not shown). Indeed, immunoblotting with an antibody recognizing the miPEP165a showed the presence of this peptide in wild-type (Col-0) seedlings, and the amount of the peptide increased when overexpressing the miPEP165a (Fig. 3a).

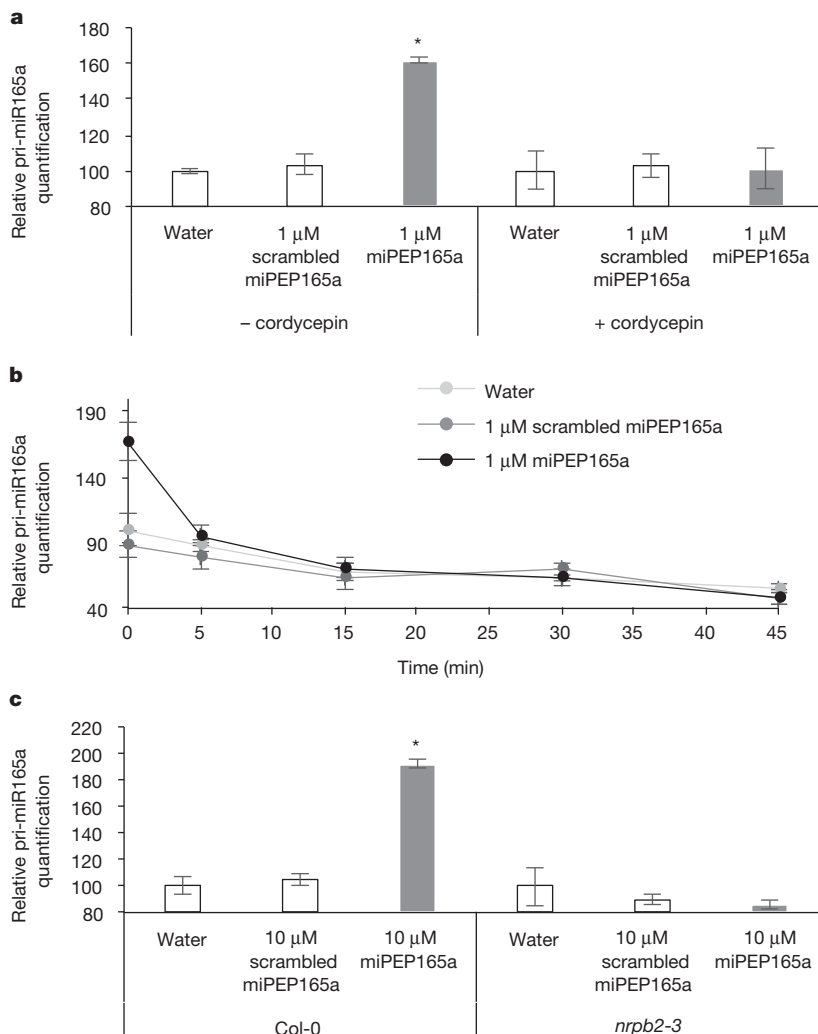


Figure 4 | Mode of action of miPEP165a.

a, Quantification of pri-miR165a in seedlings treated for 2 h with water or synthetic scrambled or miPEP165a peptides, simultaneously with or without cordycepin. **b**, Quantification of pri-miR165a in seedlings treated for 12 h with water or synthetic scrambled or miPEP165a peptides and then with cordycepin for up to 45 min. **c**, Quantification of pri-miR165a in wild-type (Col-0) or *nrpb2-3* mutant seedlings treated with water or scrambled or miPEP165a peptides. Error bars, s.e.m.; asterisks, significant difference according to a Kruskal–Wallis test, $n = 10$ seedlings, $P < 0.05$.

Treatment of *A. thaliana* seedlings with synthetic miPEP165a increased the accumulation of miR165a (Fig. 3b). Moreover, the effect of miPEP165a on accumulation of miR165a, downregulation of its target genes, and increase of root length was proportional to the dose of peptide (Fig. 3c and Extended Data Fig. 6g).

To know whether this activation of miRNAs by miPEPs is a general phenomenon, we tested five additional miPEPs and miRNAs from different miRNA families in *M. truncatula* and *A. thaliana*. In each case, application of the synthetic peptide or overexpression of the miPEP increased accumulation of the corresponding miRNA (Extended Data Fig. 7).

To understand better how miPEPs result in accumulation of their corresponding miRNAs, we analysed the expression of pri-miR165a in seedlings treated with miPEP165a for 2 h. This treatment increased the amount of pri-miR165a, unlike the treatments with water or with scrambled miPEP165a (Fig. 4a), suggesting that the miPEP either stabilized the pri-miRNA or increased its transcription. To distinguish between these two hypotheses, we treated the seedlings with miPEP165a, water or scrambled peptide for 2 h but in the presence of cordycepin, an inhibitor of RNA synthesis⁷. Cordycepin treatment completely abolished the positive effect of miPEP165a on pri-miR165a accumulation, suggesting that miPEPs activate the transcription of miRNAs (Fig. 4a). We also treated plants with miPEP165a, water or scrambled peptide, and 12 h later with cordycepin. Then we quantified the pri-miR165a at various times (Fig. 4b). As expected, the miPEP165a treatment increased the amount of pri-miR165a at time 0 (before treatment with cordycepin) compared to control roots. Upon inhibition of RNA synthesis, however, the loss of pri-miR165a was similar over time in the treated and control roots (except during the first 5 minutes), showing that the peptide does not increase the stability of pri-miR165a. Finally, we analysed the effect of miPEP165a in *nrbp2-3* mutant plants. These mutants carry a weak allele of a subunit of RNA polymerase II, which transcribes pri-miRNAs^{8,9}. We treated wild-type (Col-0) and *nrbp2-3* plants with miPEP165a, water or scrambled peptide and found no increase in the accumulation of miR165a in the mutant plants in response to the miPEP165a (Fig. 4c), further supporting the hypothesis that miPEPs are transcriptional activators of their corresponding pri-miRNAs.

The discovery of miPEPs encoded by pri-miRNAs and their effect on pri-miRNA transcription raises several questions (see Supplementary Information). Not least, how is pri-miRNA translation in the cytoplasm co-ordinated with the maturation of pri-miRNAs in the nucleus? How do miPEPs interact with the transcriptional machinery and what is the molecular basis of their specificity for their corresponding pri-miRNAs? From a practical perspective, the fact that exogenous application

of miPEPs can specifically modify plant development may have important agronomical applications.

Online Content Methods, along with any additional Extended Data display items and Source Data, are available in the online version of the paper; references unique to these sections appear only in the online paper.

Received 30 June 2014; accepted 16 February 2015.

Published online 25 March 2015.

1. Voinnet, O. Origin, biogenesis, and activity of plant microRNAs. *Cell* **136**, 669–687 (2009).
2. Lauressergues, D. *et al.* The microRNA miR171h modulates arbuscular mycorrhizal colonization of *Medicago truncatula* by targeting NSP2. *Plant J.* **72**, 512–522 (2012).
3. Combier, J. P., de Billy, F., Gamas, P., Niebel, A. & Rivas, S. Trans-regulation of the expression of the transcription factor MthAP2–1 by a uORF controls root nodule development. *Genes Dev.* **22**, 1549–1559 (2008).
4. Xie, Z. *et al.* Expression of *Arabidopsis* MIRNA genes. *Plant Physiol.* **138**, 2145–2154 (2005).
5. Carlsbecker, A. *et al.* Cell signalling by microRNA165/6 directs gene dose-dependent root cell fate. *Nature* **465**, 316–321 (2010).
6. Juntawong, P., Girke, T., Bazin, J. & Bailey-Serres, J. Translational dynamics revealed by genome-wide profiling of ribosome footprints in *Arabidopsis*. *Proc. Natl Acad. Sci. USA* **111**, E203–E212 (2014).
7. Han, M. H., Goud, S., Song, L. & Fedoroff, N. The *Arabidopsis* double-stranded RNA-binding protein HYL1 plays a role in microRNA-mediated gene regulation. *Proc. Natl Acad. Sci. USA* **101**, 1093–1098 (2004).
8. Kim, Y. J. *et al.* The role of Mediator in small and long noncoding RNA production in *Arabidopsis thaliana*. *EMBO J.* **30**, 814–822 (2011).
9. Zheng, B. *et al.* Intergenic transcription by RNA polymerase II coordinates Pol IV and Pol V in siRNA-directed transcriptional gene silencing in *Arabidopsis*. *Genes Dev.* **23**, 2850–2860 (2009).

Supplementary Information is available in the online version of the paper.

Acknowledgements This work was funded by the French ANR project miRcorrhiza (ANR-12-JSV7-0002-01), the CNRS, Paul Sabatier University Toulouse. This work is also supported by Toulouse Tech Transfer (<http://www.toulouse-tech-transfer.com>) for valorization and transfer. It was carried out in the LRSV which belongs to the Laboratoire d'Excellence entitled TULIP (ANR-10-LABX-41). We thank the GenoToul bioinformatics facility for providing computing and storage resources. We also thank J.-M. Prospéri (UMR AGAP 1334, Montpellier, France) for *M. truncatula* seeds, X. Chen (University of California, USA) for *nrbp2-3* seeds, V. Cotellet (LRSV) for help with protein analyses, C. Rosenberg (LIPM, Castanet Tolosan, France) for providing modified pCAMBIA 2200, and F. Payre and S. Plaza (CBD CNRS, Toulouse), J. Cavaillé (LBME CNRS, Toulouse) and C. Featherstone for critical reading of the manuscript.

Author Contributions J.-P.C. designed the research; J.-P.C., D.L. and G.B. designed the experiments and discussed the results; J.-P.C., D.L., J.-M.C. and Y.M. performed the experiments; J.-P.C., H.S.C. and C.D. performed bioinformatics analyses; J.-P.C. and G.B. wrote the paper.

Author Information Reprints and permissions information is available at www.nature.com/reprints. The authors declare no competing financial interests. Readers are welcome to comment on the online version of the paper. Correspondence and requests for materials should be addressed to J.-P.C. (combier@lrsv.ups-tlse.fr).

METHODS

Biological materials. *Medicago truncatula* Gaertn cv. Jemalong genotype A17 plants were cultivated on Fahraeus medium as described previously³. *Arabidopsis thaliana* Col-0 plants were cultivated on Murashige and Skoog (MS)-based medium containing 4.4 g l⁻¹ MS base (Sigma), 10% sucrose (Sigma), 6 g l⁻¹ agarose (Sigma), pH 5.8.

Plasmid constructs. Plasmids were obtained by using pPEX or pBIN³ vectors or Golden Gate cloning strategy¹⁰. Expressions in tobacco leaves were performed using 35S promoter. pPEX and pBIN plasmids were used for overexpression studies, by cloning the fragment of interest with XhoI-NotI and ClaI-BamHI, respectively (see Extended Data Table 3 for primers used). A modified pCambia2200 binary vector¹¹ was used with the Golden Gate strategy for other cloning. The fragments to be cloned were flanked by *BsaI* restriction sites during the PCR amplification step. One-step digestion–ligation reactions were carried out with 100 ng modified pCambia, 100 ng of each PCR fragment, 1 µl 10× ligase buffer (Promega), 2.5 U T4 DNA ligase (Promega), 2.5 U *BsaI* (NEB), in a final volume of 10 µl and incubated at 37 °C for 30 min and 16 °C for 30 min and repeated once. A final incubation step at 50 °C for 20 min was used to cleave any remaining undigested cloning vector. In studies of miPEP171b and miPEP165a, 2.3 kilobase (kb) and 4 kb of promoter sequences were used for GUS analyses, respectively.

Plant transformation. Composite plants of *M. truncatula* A17 with *Agrobacterium rhizogenes*-transformed roots were obtained by the procedure described previously³. Tobacco leaf transformation was performed as described previously³. *A. thaliana* were transformed according to ref. 12. Transformants were selected on MS medium (4.4 g l⁻¹ MS base (Sigma), 10% sucrose (Sigma), 6 g l⁻¹ agarose (Sigma), pH 5.8) supplemented with 25 mg l⁻¹ kanamycin.

Histochemical staining. GUS staining was performed as described previously³. The samples were observed with an Axiozoom V16 microscope (Zeiss).

Expression analyses. miRNA quantification was performed by northern blot analyses², or by stem-loop quantitative reverse transcription (qRT)–PCR¹³. In brief, RNAs were extracted by using the TRI Reagent (Molecular Research Center, Inc.) following the manufacturer's instructions, except that the RNAs were precipitated with three volumes of ethanol. RNAs were reverse-transcribed using a specific reverse-transcription-primer stem-loop in combination with hexamers, adapted from ref. 13. One microgram of RNAs was added to stem loop primer (0.2 µM), hexamers (500 ng), reverse transcription buffer (1×), SSIII (Invitrogen) (1 U), dNTPs (0.2 mM each), and dithiothreitol (0.8 mM) in a total volume of 25 µl. Gene expression was measured by qRT–PCR (see Extended Data Table 3 for primers used) and performed as described previously³. Actin was used as housekeeping gene to normalize qRT–PCR analyses on *A. thaliana* (See Extended Data Table 3). For northern blotting analyses, U6, which is a non-coding small nuclear RNA was used as a control for equal loading. Levels of expression in Fig. 4a, c for the controls were set at 100. For all the qPCR, each biological sample has two technical replicates.

Statistical analyses. The mean values of relative gene expression, lateral root production or root length were compared by using Student's *t*-test (when *n* > 30) or the Kruskal–Wallis test (when *n* < 30). In each case, *n* represents independent biological replicates. Error bars represent the standard error of the mean (s.e.m.). Asterisks indicate significant differences (*P* < 0.05). No statistical methods were used to predetermine sample size.

Peptide assays. Peptides were synthesized by Smartox (<http://www.smartox-biotech.com>) and dissolved at 10 mM in water (miPEP164a, miPEP65a), in 10% acetic acid (v/v) (miPEP169d), or in 40% water, 50% acetonitrile and 10% acetic

acid (v/v/v) (miPEP171b). Plants were treated with concentrations from 0.01 to 10 µM peptide diluted in the agar growth medium or in solution in water (for Fig. 4a, b).

Sequences. miPEP164a: MPSWHGMVLLPYVKHSTHSTHTHTHNYGCACE LVFH; miPEP165a: MRVKLFQLRGMLSGSRL; scrambled miPEP165a: SMKQ RVLLGRLSIFGLMR; miPEP169d: MVKESFMERLKVR; miPEP171b: MLLHRLS KFCKIERDIVYIS; scrambled miPEP171b: LIVSHLYSEKFDCMRKILRI.

Antibodies. Polyclonal antibodies against full-length miPEP165a and miPEP171b were obtained by inoculating rabbits (<http://www.agrobio.com>). Antibodies were purified by affinity chromatography on columns containing the appropriate peptide.

Immunoblots. Total protein extracts were obtained as described previously³, and 50 µg were loaded and separated by SDS PAGE. Transfer was performed in phosphate buffer overnight at 4 °C and at 15 V, and the membrane was incubated for 45 min at room temperature in 0.2% (v/v) glutaraldehyde. Primary antibodies were used at 1:1,000 (v/v) dilution and HRP-conjugated goat anti-rabbit IgG (<http://www.agrobio.com>) was used as secondary antibody at 1:40,000 (v/v) dilution. Immunoblotting of tubulin was performed as a control for equal loading (Fig. 3a).

Immunohistochemistry. Hairy roots and plantlets of *M. truncatula* were fixed for two hours in 4% (v/v) formalin in 50 mM cacodylate buffer (pH 7.2). Then they were embedded in 5% low melting-point agarose dissolved in water. Semi-thin sections (100 µm) were prepared and placed on Teflon-coated well slides in phosphate buffer for immunology (PBi: 0.1 M potassium phosphate buffer pH 7.5). The sections were blocked by incubating in PBi containing 2% Tween (PBiT) and 1% bovine serum albumin for 2 h (PBiT–BSA), then incubated overnight (12 h) at 4 °C with primary antibody diluted 1:50 (v/v) in PBiT–BSA. They were then washed five times with PBiT over the course of 3 hours and incubated at room temperature for 2 hours with a goat anti-rabbit IgG coupled to Alexa Fluor 633 (Molecular Probes) diluted 1:1,000 (v/v) in PBiT–BSA. Finally, the slides were washed in PBi for 1 hour, mounted in Citifluor (antifading mounting medium) and observed by confocal microscopy on a LeicaTCS SP2 laser scanning confocal microscope. The signal obtained from controls with pre-immune serum instead of primary antibody, or in the absence of primary antibody, were subtracted from the signal obtained with the specific antibody.

RNA stability. Two-week-old plants grown vertically on solid MS medium were transferred into wells of six-well plates containing 1 ml liquid MS medium. Simultaneously or after 16 h incubation with 1 µM miPEP165a, the plants were treated with 100 µg ml⁻¹ cordycepin (Sigma) and harvested after various times for RNA extraction and quantification. Experiments were repeated three times.

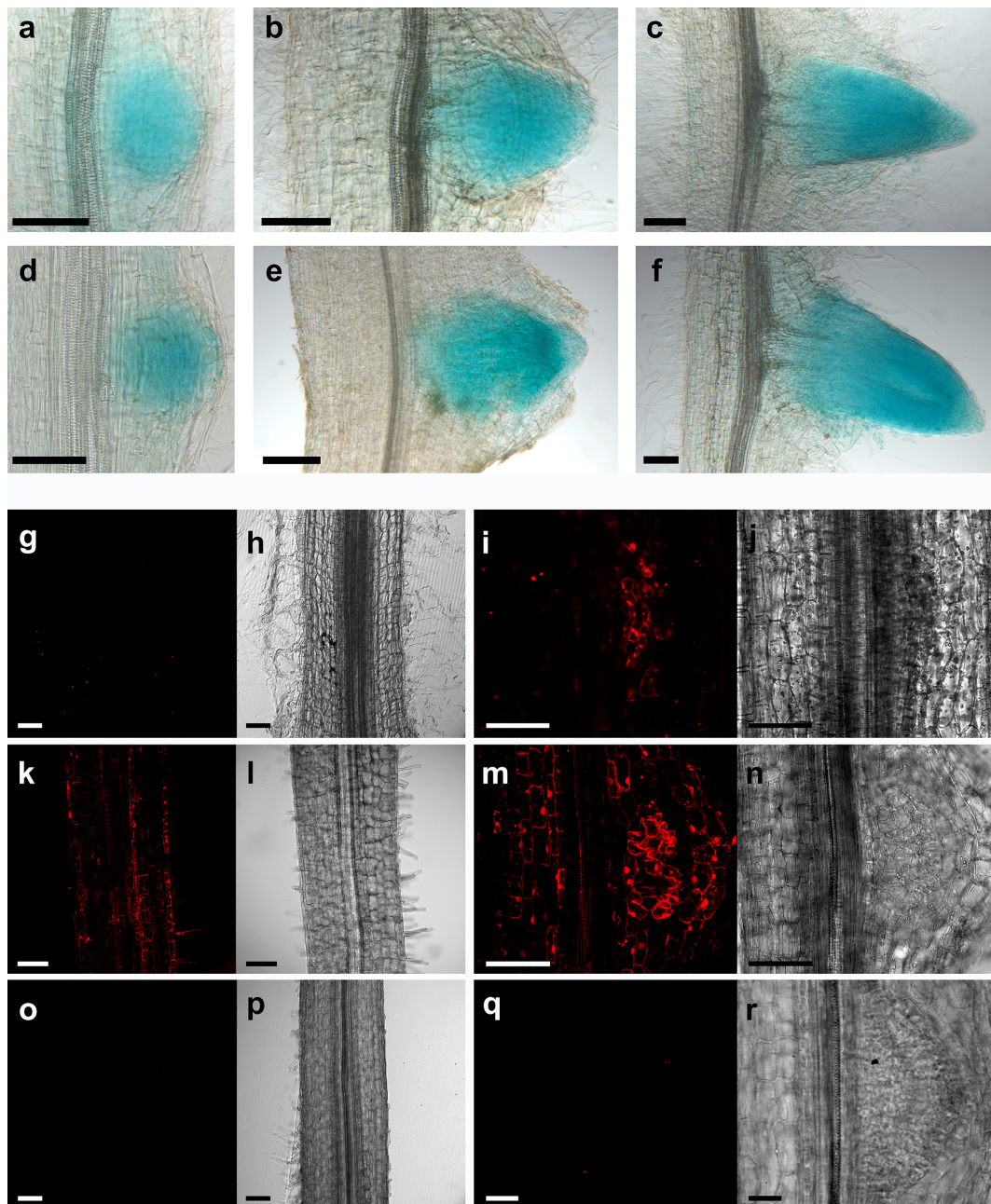
RACE–PCR. For pri-miRNA 5' end identification, RACE–PCR was carried out following the manufacturer's instructions (FirstChoiceRLM–RACE kit, Ambion). For pre-miRNA 5' end identification, the Calf Intestinal Phosphatase treatment was omitted.

- Engler, C., Kandzia, R. & Marillonnet, S. A one pot, one step, precision cloning method with high throughput capability. *PLoS ONE* **3**, e3647 (2008).
- Fliegmann, J. et al. Lipo-chitooligosaccharidic symbiotic signals are recognized by LysM receptor-like kinase LYR3 in the legume *Medicago truncatula*. *ACS Chem. Biol.* **8**, 1900–1906 (2013).
- Clough, S. J. & Bent, A. F. Floral dip: a simplified method for *Agrobacterium*-mediated transformation of *Arabidopsis thaliana*. *Plant J.* **16**, 735–743 (1998).
- Mestdagh, P. et al. High-throughput stem-loop RT-qPCR miRNA expression profiling using minute amounts of input RNA. *Nucleic Acids Res.* **36**, e143 (2008).

ATTGGTCAAACATACATACAGTAGCTAGCTGGTTTCATTATCCACTATG¹CTTCTTCATAGGCTCTCC
M L L H R L S
AAATTTTGCAAAATTGAAAGAGACATAGTATATATATCTTAGCAAGGAGAAATTCAGGATATTGAGGATG²
K F C K I E R D I V Y I S M
AAGATTGAAGAGTAA TCAGTGATGAAGAAAGCAAGCAAGGTA TTGGCGCGCCTCAATTTGAATACATGGCT
K I E E
ATAAAAAATGCATCATATCAGCCATGTAGTTTGATTGAGCCGCGTCAATATCTTGTTCATCTCCAA//

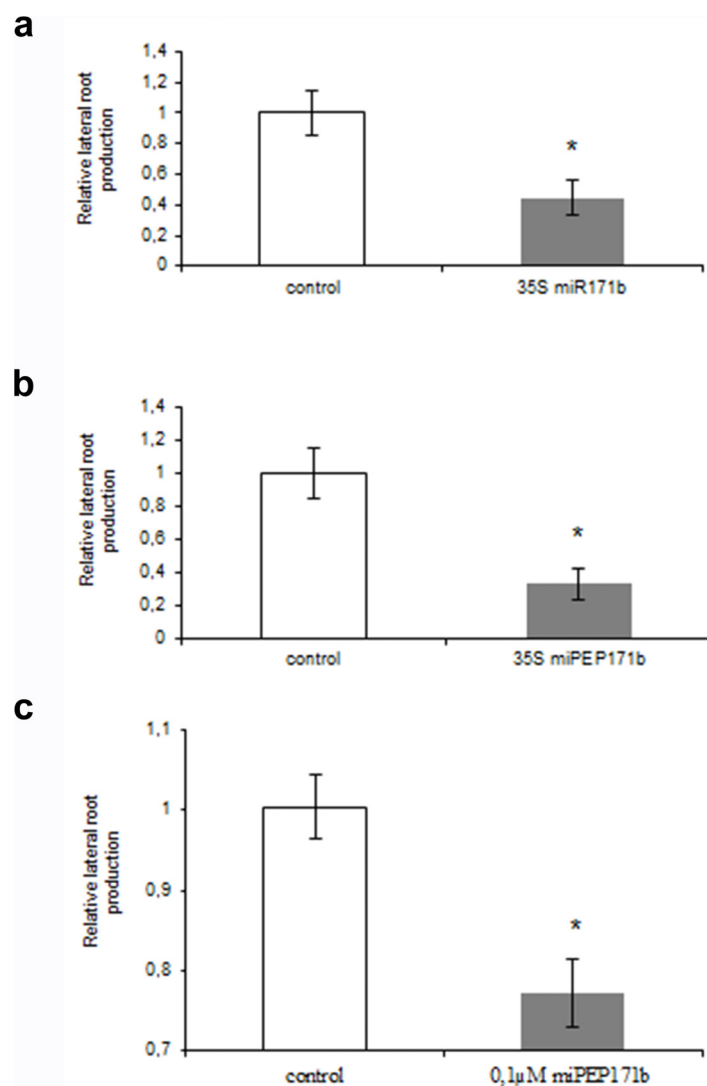
Extended Data Figure 1 | Characterization of the *M. truncatula* miPEP171b. The 5' part of the pri-miR171b, as identified by 5' RACE-PCR analysis. The short putative ORFs are in blue, the miR171b* in green, and the mature miR171b in red. The two first ATG start codons of the pri-miR171b

are underlined, and the sequences of their corresponding peptides are shown below. The black vertical line indicates the 5' end of the pre-miR171b precursor, identified by 5' RACE-PCR.



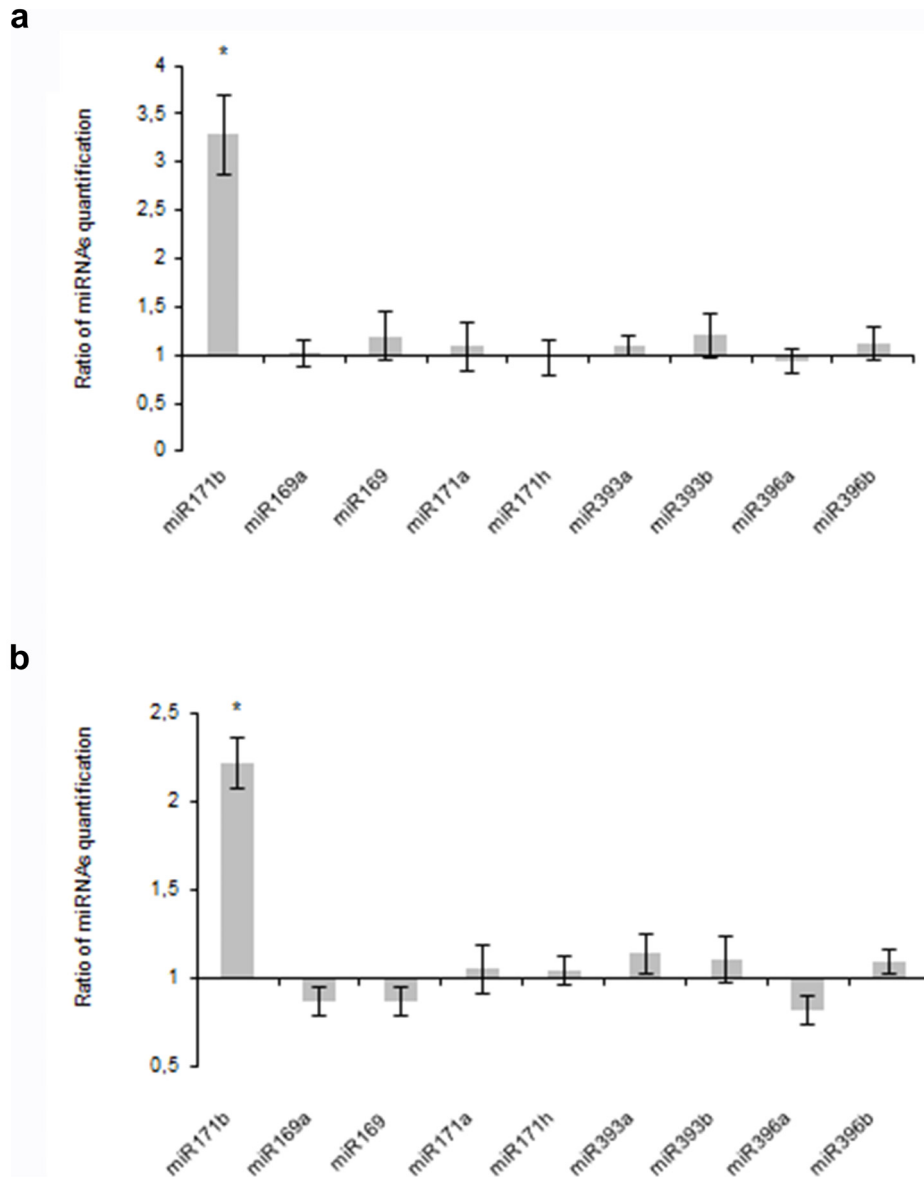
Extended Data Figure 2 | Expression of miPEP171b in *M. truncatula* roots. **a–c**, Staining for GUS activity (blue) showing expression of the miR171b at different stages of lateral root development. **d–f**, Staining for GUS activity (blue) showing expression of the miPEP171b at different stages of lateral root development. **g–r**, Immunolocalization of miPEP171b. Confocal immunofluorescence microscopy of endogenous miPEP171b (red) in the main roots (**g**) and lateral root primordia (**i**) of wild-type plants, and their corresponding bright-field images (**h**, **j**). Confocal immunofluorescence

microscopy of miPEP171b (red) in main roots (**k**) and lateral root primordia (**m**) in roots overexpressing miPEP171b, and their corresponding bright-field images (**l**, **n**). Controls for immunofluorescence staining of main roots (**o**) and lateral root primordia (**q**) of wild-type plants, and their corresponding bright-field images (**p**, **r**), in which the primary antibody was omitted (scale bars, 100 μ m). One representative experiment of nine (**g–j**), four (**k–n**) or seventeen (**o–r**) performed is shown.



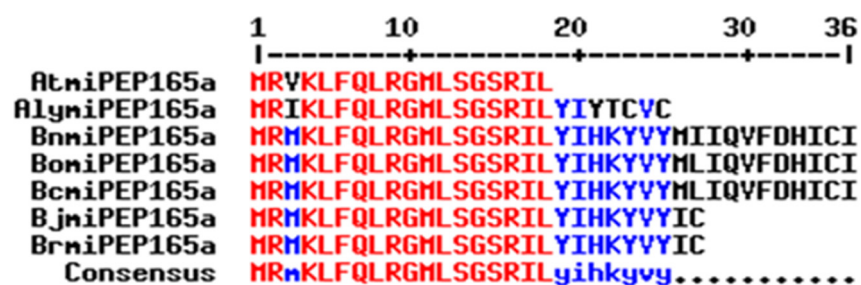
Extended Data Figure 3 | Effect of an upregulation of the miR171b on root development in *M. truncatula*. **a**, Relative production of lateral roots in roots overexpressing the pri-miR171b compared to the production in control roots. **b**, Relative production of lateral roots in roots overexpressing the miPEP171b compared to the production in control roots. **c**, Relative

production of lateral roots in plants treated with 0.1 μ M miPEP171b synthetic peptide (0.1 μ M miPEP171b) compared to the production in roots treated with control solvent (control). Error bars represent s.e.m., asterisks indicate a significant difference between the overexpressing roots and the control according to Student's *t*-test ($n = 100$ independent plants, $P < 0.05$).



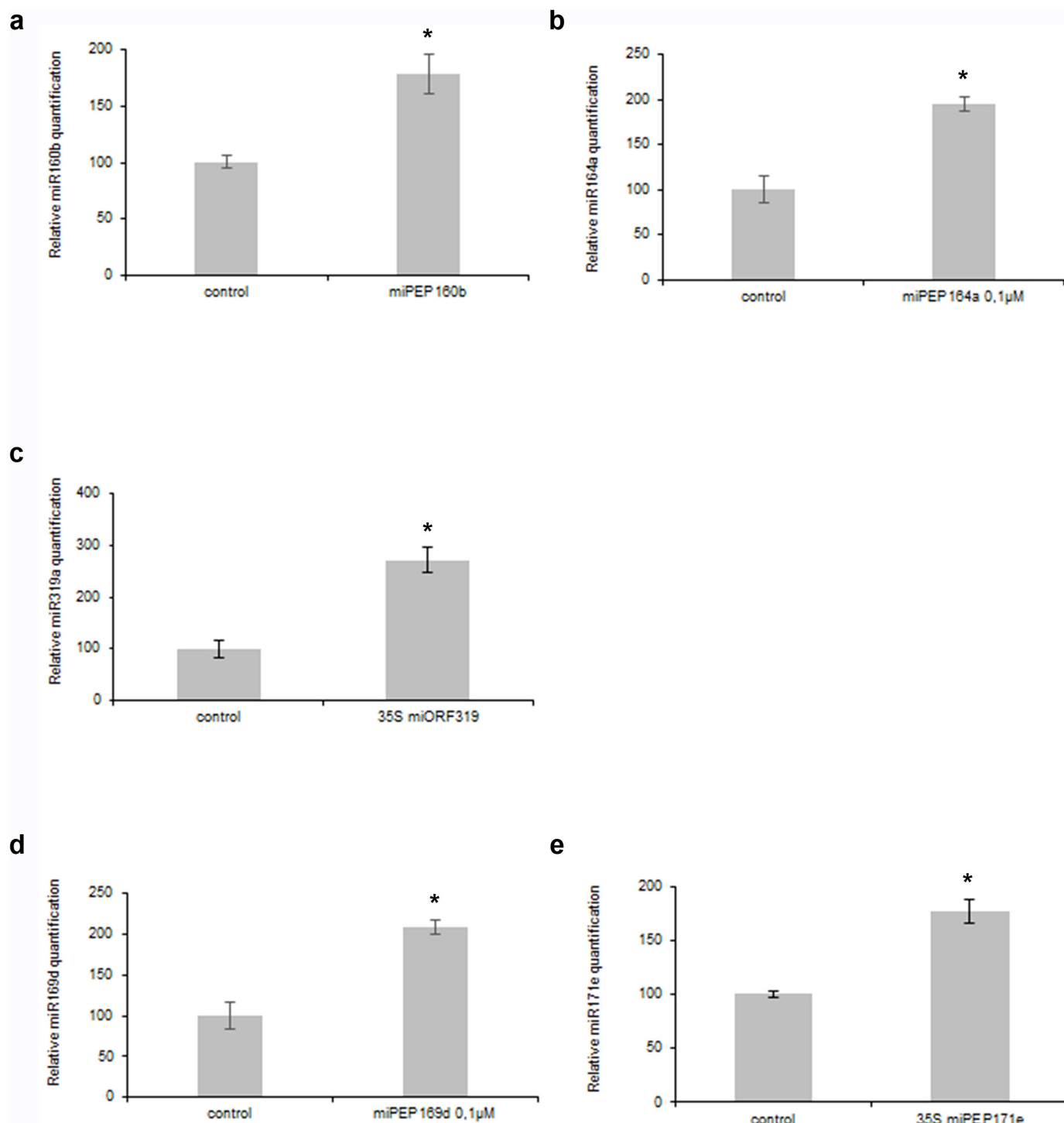
Extended Data Figure 4 | Effect of miPEP171b on the expression of various miRNAs in *M. truncatula*. **a**, Effect of overexpression of miPEP171b. **b**, Effect of exogenous treatment with 0.1 μ M of the synthetic miPEP171b. Histograms represent the relative expression of each miRNA in roots overexpressing

miPEP171b compared to wild-type roots (**a**) or in roots treated with the peptide compared to the roots treated with solvent (**b**). Error bars represent s.e.m., asterisks indicate a significant difference between the treatment and the control according to a Kruskal–Wallis test ($n = 10$ independent roots, $P < 0.05$).



Extended Data Figure 5 | Alignment of miPEP165a amino acid sequences of seven species of Brassicales using MultAlin. MultAlin available at <http://multalin.toulouse.inra.fr/multalin/multalin.html>. At, *Arabidopsis thaliana*; Aly, *Arabidopsis lyrata*; Bn, *Brassica napus*; Bo, *Brassica oleracea*;

Bc, *Brassica carinata*; Bj, *Brassica juncea*; Br, *Brassica rapa*. Red represents homology in all seven species; blue represents homology in most of the species. Upper-case letters denote high-consensus sequence; lower-case letters denote low-consensus sequence.



Extended Data Figure 7 | Effect of various miPEPs from *Arabidopsis thaliana* and *Medicago truncatula* on the expression of their corresponding miRNA. a–c, miPEPs from *A. thaliana*. a, Expression of miR160b in response to overexpression of miPEP160b. b, Expression of miR164a in response to treatment with 0.1 μ M of miPEP164a. c, Expression of miR319a in response to overexpression of miPEP319a. d–e, miPEPs from *M. truncatula*. d, Expression

of miR169d in response to treatment with 0.1 μ M of miPEP169d. e, Expression of miR171e in response to overexpression of miPEP171e. Error bars represent s.e.m., asterisks indicate a significant difference between the treatment and the control according to a Kruskal–Wallis test ($n = 10$ independent roots or tobacco leaves, $P < 0.05$).

Extended Data Table 1 | DNA polymorphism analysis of various regions of the pri-miR171b in 284 ecotypes of *M. truncatula*

	size	# SNPs	# mutations	% SNP	# haplotypes
Promoter pri-mir171b	1127	91	100	8.07	161
5' pri-miR171b	129	4	4	3.1	5
miPEP171b	62	2	2	3.22	3
Pre-miR171b	118	1	1	0.85	2
miR171b+miR171b*	42	0	0	0	1
3' pri-miR171b	259	39	42	15.06	89

A haplotype is defined as a sequence that differs by at least one SNP from the other haplotypes.

Extended Data Table 2 | List of putative miPEPs identified in *A. thaliana* (in which the putative start codon is ATG)

name	sequence	size (aa)	size (MW)
miPEP156a	MFCSIQCVARHLFPLHVREIKKATRAIKKGKTL	33	3824
miPEP156c	MKDNFPLLLRL	11	1359
miPEP156e	MIYINKYGSISAVEDD	16	1818
miPEP156f	MSQR	4	520
miPEP157c	MMLHITHRFESDVGC	15	1776
miPEP157d	MLYV	4	524
miPEP159a	MTWPLLSLSFLLSKYV	16	1898
miPEP159b	MFYLS	5	659
miPEP160a	MFCLLIPIFS FVFSNRLRLQEQ	24	2936
miPEP160b	MFSPQ	5	608
miPEP160c	MEMRRGLVYNNIYI	14	1790
miPEP161	MKIPLELPKL	10	1199
miPEP162a	MVSGQEDSWLKLSLCLFLSLDLSLI	27	3045
miPEP162b	MFLLIFLRLIMICVCSSTDFLRSVNYFCLFIYDL	34	4114
miPEP163	MSTTQEHRS	9	1076
miPEP164a	MPSWHGMVLLPYVKHTHASTHTHNIYGCACELVFH	37	4256
miPEP164b	MMKVCDEQDGEAGHVHY	17	1949
miPEP165a	MRVKLFQLRGMLSGSRIL	18	2105
miPEP166a	MLDLFRSNRRIEPSDFRFD	19	2372
miPEP166b	MRDR	4	576
miPEP166c	MKKRITRINLEEQIKKTLDDSRTRLHSP	28	3407
miPEP166d	MKKIGSIDSF	10	1125
miPEP167a	MNRKISLSLS	10	1148
miPEP167b	MMGCFVGF	8	891
miPEP169a	MTCRFK	6	784
miPEP169c	MPHTNLKDLFIFS PNVFFSFAIYLHNSWNKNYIHKRENFHNTS FALIFFSSIMS INYG	59	7110
miPEP169h	MVT	3	349
miPEP169l	MRHES	6	786
miPEP169n	MKCMKKRGLTWRKASCLVAKDDLPLDLRLHDSISNSCILDYYTF	45	5315
miPEP170	MFRESL	7	879
miPEP171a	MNLLKKEQRQRQSRIGSHCIASLVLDGVMKKI	34	4057
miPEP171b	MVLSGKLT	9	995
miPEP171c	MLSLSHFHIC	10	1187
miPEP172a	MASKIW	6	734
miPEP172b	MCTYYLILNKYF	12	1621
miPEP172c	MFPKWCRLES	11	1367
miPEP172e	MGSLSLFKSQLEIIMLLLSLSK	22	2452
miPEP319a	MNIHTYHLLFPSLVFHQSSEVPNALS LHIHTYEYIIIVVIDPFRITLAFR	50	5917
miPEP319b	MVPQINLWSSRVI LKIRIDSSTHREEDHCIONHKHGLSFI FFF	43	5120
miPEP394a	MSLQFYERVSFKNTVK	16	1977
miPEP395c	MTEQEEESQMST	12	1429
miPEP395e	MYLQYIDNVI SIYSNNRRVGRMFSRVPLSTSLEIQFFIK	39	4700
miPEP396a	MTLSVFFHSFLELQNFRRFFFSFDISYA	29	3636
miPEP397b	MSKEIFFSPGFE	12	1418
miPEP399b	MKRNM	5	678
miPEP399c	MSLAKGELPCHCFRINTVYNRFC	23	2703
miPEP399d	MQCEI	5	622
miPEP403	MFCA	4	470
miPEP447a	MVMAHH	6	724
miPEP447b	MLLIIVELVL	10	1155

aa, amino acids; MW, molecular weight.

Extended Data Table 3 | List of primers used

name	sequence
promiR171b 5'	GGGCTCTCCATGGGCTGTTAGATCCAACTTCGG
promiR171b 3'	GGGCTCTCCATGGGCTGTTAGATCCAACTTCGG
promiR171b 3' ATG1	22GGTCTCgACACAAGCATAGTGGAAATGAAACC
promiR171b 3' ATG2	2222GGTCTCgCCATCTTCATCCTCAATATCCTAATTC
promiR171b 3' fusionORF1	22GGTCTCgACACAGATATATATCTATGTCTCTTTCA
miR171b5'	222GGTCTC C TAGC TTGGTCAAACATACATACAGTAGCACTAG
miR171b 3'	222GGTCTCgCGTAAATTTGTACTGATTGAATGAAATGGTACAC
miORF171b5'	TCAGTCCGCTCGAGATGCTTCTTCATAGGCTCTCC
miORF171b3'	AAGGAAAAAAGCGGCGCGCTAAGATATATATCTATGTCTCTTTCAA
miORF171b5'ATT	TCAGTCCGCTCGAGATTCTTCTTCATAGGCTCTCC
miORF171b5'delta orf	CAAGGAGAAATTCAGGATATTGAGGATGA
miORF171b3'delta orf	TCATCTCAATATCTGAATTTCTCTTGTAGTGGAAATAATGAAACCAGCTAG
miORF5' synonymous	AAGTTCTGTAAGATAGAGCGGATATTGTTTACATTAGCTAGCAAGGAGAAATTCAGGATATTGAGGATGA
miORF3' synonymous	CAATATCGCGCTCTATCTTACAGAACTTACTTAAGCGGTGTAATAACATAGTGGAAATAATGAAACCAGCTAG
miR160b5'	222GGTCTCgTAGCACTCATAACTCTCCCCAAATTC
miR160b3'	222GGTCTCgCGTAGAAAGAATGTTGCGAAAAAC AATG
miORF160b5'	TAGCATGTTTTCCCTCAATGA
miORF160b3'	cgt2TCATTGAGGGGAAAAACAT
miR319a5'	tcacgAGAGAGAGCTTCTTGAGTC
miR319a3'	tcgggatccAGAGGGAGCTCCCTTCAGT
miORF319a5'	tcacgATGAATATACATACATACCATCAT
miORF319a3'	tcgggatccTCTAAAAGCTAAAGTGATTCTAAA
miR171e5'	TCAGTCCGCTCGAGGAATAAGTGAATATTATCGATATTT
miR171e3'	AAGGAAAAAAGCGGCGCAAGTGATATTGGCGCGGCT
miORF171e5'	tcacgATGATGGTGTGTTGGGAAGCC
miORF171e3'	tcgggatccTACATGTAATCCGCTTCCGG
promiR165aBsal5	aGGTCTCCAAATttaaactgtca gtgc atg gat gt
miORF165a fusion GTG Bsal 3	aGGTCTCgACACattcacaatttt ttgtt gta ga gag
miORF165a fusion CTG Bsal 3	aGGTCTCgACACtagcagattcac aa atttt ttgtt g
miORF165a fusion ATG Bsal 3	aGGTCTCgACACcctcatgataatcg atctt agc a
miORF165aBsal5	tcacgATGAGGGTTAAGCTATTTAGT
miORF165aBam3	tcgggatccTAATATCTCGATCCAGACAAC
Mtubi5	GCAGATAGACACGCTGGGA
Mtubi3	AACTCTTGGGCAGGCAATAA
miR171bq5	GTCGTATCCAGTGCAGGGTCCGAGGTATTGCACTGGATACG ACGATATT
miR171bq3	TGCGTTGATTGAGCCGCGTC
LOM1q5	AATGATGGATGCTTCGGTTC
LOM1q3	TGTTTCTGCTGCTGATGTC
LOM2q5	CTGAAACTGATGAGCCGACA
LOM2q3	TGGATATTTGCATGGCTCAA
pri-miR165a5	CTTGCGCAAAATACAAAAGC
pri-miR165a3	GCCATGCAAGAAAGATTCAA
AtPHVq5	GCAACTGCAGTGGAAATAGCA
AtPHVq3	GCGACCTTCATGGGTCTAA
AtPHBq5	CTCAGCATCAGCAACGTGAT
AtPHBq3	AACTCTGCTAGGGCTCTCTC
AtREVq5	TCACAACCTCTCAGCATTCG
AtREVq3	ACCCAATCAACAGCAGTTCC
Atactine2F	GGTAACATTGTGCTCAGTGG
Atactine2R	CTCGGCTTGAGATCCACA